Neutrino Annihilation in Stellar Magnetic Fields

C.J. Benesh and C.J. Horowitz,
Nuclear Theory Center, Indiana University,
Bloomington, IN 47405

February 1, 2008

Abstract

The potential enhancement of the cross section $\nu\bar{\nu} \rightarrow e^+e^-$ in the presence of a magnetic field is of critical interest for the study of supernovae and as a possible mechanism for gamma ray bursts. While parity violation(PV) in this reaction in free space is forbidden by CP, the presence of a CP non-invariant background gas of electrons creates an asymmetry in the cross section which may contribute to the asymmetry of a supernova and the natal velocities of neutron stars. We calculate the cross section in the presence of fields as high as $B = 10^{16}$G and find no significant enhancement of the cross section with magnetic field strength. By studying the systematics of our results as a function of environmental variables(field strength, density,temperature), we extrapolate the relative strength of the parity violating terms to the weak field limit, and find the parity violation is insufficient to provide the "kick" required to explain the observed velocities of neutron stars.

1 Introduction

Violent stellar events, such as supernovae and neutron star collisions, release tremendous amounts of energy, primarily in the form of neutrinos[1]. In regions of low density, the annihilation process $\nu\bar{\nu} \rightarrow e^+e^-$ has been proposed as a source of energy to restart the shock wave in core collapse supernovae[2], and as a means of generating an energetic e^+e^- plasma for gamma ray bursts[3]. Since detailed calculations of supernova and gamma ray burst scenarios indicate that the annihilation rate is too low[4], it has been suggested that the star's magnetic field will act as a catalyst for the reaction by eliminating some kinematical constraints on the e^+e^- pair[3]. The case for such an enhancement is motivated by studies of pair creation ($\gamma \rightarrow e^+e^-$ and $\gamma \rightarrow \gamma\gamma$)[5] and the neutrino synchotron process ($\nu \rightarrow \nu e^+e^-$[6] [7]), where processes that are kinematically disallowed in the vacuum are made possible by the exchange of momentum between the e^+e^- pair and the magnetic field. The central role of the magnetic field in these processes is reflected in the sensitivity of the cross sections to the field strength. Significantly, this enhancement does not seem to occur in processes that are kinematically allowed in the absence of the field[8].

As an added bonus, the magnetic field provides a preferred direction in space, opening the way for parity violating effects to produce an asymmetry in neutrino cross sections. The asymmetries, which have been calculated for $\nu - e$ scattering[7][9] and ν-nucleus elastic scattering[10], provide a mechanism for producing asymmetric supernova explosions, either directly or by asymmetrically heating the surrounding matter. Such asymmetric explosions have been proposed as a means of producing the observed large velocities of pulsars[6].

In this paper, we calculate the $\nu\bar{\nu}$ annihilation for a variety of magnetic field strengths, densities, and temperatures similar to those found in supernovae. Our formalism[8][9][10], is detailed in the next section, while our results and their implications for astrophysics are left to the concluding section.

2 Formalism

We consider the process for $\nu\bar{\nu}$ annihilation in the presence of a magnetic field of strength $\mathbf{B}$ in the z direction, using the four point interaction

$$L_{int} = \frac{G_F}{\sqrt{2}} \int d^4x \, \bar{\nu}(x)\gamma_\alpha(1-\gamma_5)\nu(x) \, \bar{e}(x)\gamma^\alpha(C_V - C_A\gamma_5)e(x), \tag{1}$$

where $G_F = 1.13 \times 10^{-11}$ MeV^{-2} is the Fermi coupling strength, $C_V = 2\sin^2\theta_W \pm \frac{1}{2}$, $C_A = \pm\frac{1}{2}$ with the plus sign for electrons and the minus for μ or τ neutrinos, and $\sin^2\theta_W \approx .223$.

The wavefunctions of the electron-positron pair are obtained by solving the Dirac equation in Landau gauge ($A_x = -By$)[13]

$$
\begin{aligned}
\Psi^{e^-}_{(p_x,p_z,n,\sigma)}(\mathbf{x},t) &= \frac{e^{ip_x x}e^{ip_z z}e^{-i\epsilon t}}{\sqrt{L_x L_z}}\begin{pmatrix}\alpha C H_{n-1}(\xi)\\ -\sigma\alpha D H_n(\xi)\\ \sigma\beta C H_{n-1}(\xi)\\ -\beta D H_n(\xi)\end{pmatrix},\\
\Psi^{e^+}_{(p'_x,p'_z,m,\sigma')}(\mathbf{x},t) &= \frac{e^{-ip'_x x}e^{-ip'_z z}e^{-i\epsilon' t}}{\sqrt{L_x L_z}}\begin{pmatrix}\beta' D' H_{m-1}(\xi')\\ -\sigma'\beta' C' H_m(\xi')\\ -\sigma'\alpha' D' H_{m-1}(\xi')\\ \alpha' C' H_m(\xi')\end{pmatrix},
\end{aligned}
\tag{2}
$$

where $\begin{pmatrix}\alpha\\ \beta\end{pmatrix} = \frac{1}{\sqrt{2}}(1 \pm \frac{m_e}{\epsilon})^{\frac{1}{2}}$, $\begin{pmatrix}C\\ D\end{pmatrix} = \frac{1}{\sqrt{2}}(1 \pm \frac{\sigma p_z}{(\epsilon^2-m^2)^{\frac{1}{2}}})^{\frac{1}{2}}$, $\sigma = \pm 1$ is the electron's helicity, $H_n(\xi)$ is the normalized solution of a one dimensional harmonic oscillator with $\xi = \sqrt{eB}(y - \frac{p_x}{eB})$, and the energies of the Landau levels are given by $\epsilon = \sqrt{p_z^2 + 2eBn + m_e^2}$. For the positron spinor, the primed quantities are obtained from the unprimed by replacing $\epsilon \to \epsilon'$, $p_i \to p'_i$, and $\xi' = \sqrt{eB}(y + \frac{p'_x}{eB})$.

The differential cross section for the annihilation process is given by

$$
d\sigma = \frac{G_F^2 L_x L_z}{4\pi k_1 \cdot k_2 V} C_{\mu\nu} A^{\mu\nu} \delta(Q_0 - \epsilon - \epsilon')\delta(Q_z - p_z - p'_z)\delta(Q_x - p_x - p'_x) dp_x dp_z dp'_x dp'_z, \tag{3}
$$

where $Q^\mu = k_1^\mu + k_2^\mu$, with $k_1(k_2)$ the (anti-)neutrino momentum, $V = L_x L_y L_z$ is a normalization volume,

$$
C^{\mu\nu} = k_1^\mu k_2^\nu + k_1^\nu k_2^\mu - g^{\mu\nu} k_1 \cdot k_2 + i\epsilon^{\mu\nu\alpha\beta} k_{1\alpha} k_{2\beta}, \tag{4}
$$

and $A^{\mu\nu} = \sum_{\sigma\sigma'} S^\mu S^{*\nu}$ is the spin-summed product of the current matrix elements of the electron. Neglecting the electron mass, the matrix elements are given by

$$
\begin{aligned}
S^0 &= \frac{(1-\sigma\sigma')}{2}(C_V - C_A\sigma)(-DC'F_{nm} + CD'F_{n-1,m-1})\\
S^1 &= \frac{(1-\sigma\sigma')}{2}(C_V - C_A\sigma)(-DD'e^{i\phi}F_{n,m-1} - CC'e^{-i\phi}F_{n-1,m})\\
S^2 &= -i\frac{(1-\sigma\sigma')}{2}(C_V - C_A\sigma)(-DD'e^{i\phi}F_{n,m-1} + CC'e^{-i\phi}F_{n-1,m})\\
S^3 &= \frac{(1-\sigma\sigma')}{2}(C_V - C_A\sigma)\sigma(DC'F_{nm} + CD'F_{n-1,m-1}),
\end{aligned}
\tag{5}
$$

where

$$
F_{nm} = \left(\frac{n_<!}{n_>!}\right)^{\frac{1}{2}} \left(\frac{(n-m)}{|n-m|}\sqrt{\frac{Q_\perp^2}{2eB}}\right)^{n_< - n_>} e^{\frac{-Q_\perp^2}{4eB}} e^{i(m-n)\phi} L_{n_<}^{n_> - n_<}\left(\frac{Q_\perp^2}{2eB}\right), \tag{6}
$$

with L_n^α a generalized Laguerre polynomial[12] and $\tan\phi = Q_y/Q_x$. Here $n_>$ is the greater of n and m.

To simplify the remainder of the calculation, we choose coordinates such that $Q_y = 0$. In this system, the non-zero components $A_{\mu\nu}$ are given by

$$
\begin{aligned}
A_{00} &= \frac{1}{2}\Big[(C_V^2 + C_A^2)\Big((1 + v_e v_p)(|F_{nm}|^2 + |F_{n-1,m-1}|^2) + 2v_n v_m F_{nm} F_{n-1,m-1}|_{\phi=0}\Big) \\
&\quad -2C_V C_A(v_e + v_p)\Big(|F_{n-1,m-1}|^2 - |F_{nm}|^2\Big)\Big] \\
A_{11} &= \frac{1}{2}\Big[(C_V^2 + C_A^2)\Big((1 - v_e v_p)(|F_{n,m-1}|^2 + |F_{n-1,m}|^2) - 2v_n v_m F_{n,m-1} F_{n-1,m}|_{\phi=0}\Big) \\
&\quad +2C_V C_A(v_e - v_p)\Big(|F_{n-1,m}|^2 - |F_{n,m-1}|^2\Big)\Big] \\
A_{22} &= \frac{1}{2}\Big[(C_V^2 + C_A^2)\Big((1 - v_e v_p)(|F_{n,m-1}|^2 + |F_{n-1,m}|^2) + 2v_n v_m F_{n,m-1} F_{n-1,m}|_{\phi=0}\Big) \\
&\quad +2C_V C_A(v_e - v_p)\Big(|F_{n-1,m}|^2 - |F_{n,m-1}|^2\Big)\Big] \\
A_{33} &= \frac{1}{2}\Big[(C_V^2 + C_A^2)\Big((1 + v_e v_p)(|F_{n,m}|^2 + |F_{n-1,m-1}|^2) - 2v_n v_m F_{n,m} F_{n-1,m-1}|_{\phi=0}\Big) \\
&\quad -2C_V C_A(v_e + v_p)(|F_{n-1,m-1}|^2 - |F_{n,m}|^2)\Big] \\
A_{01} &= A_{10} = \\
&\quad \frac{1}{2}\Big[-(C_V^2 + C_A^2)\Big(v_n(F_{n,m-1}F_{n-1,m-1} + F_{n-1,m}F_{n,m}) + v_m(F_{n,m-1}F_{n,m} + F_{n-1,m}F_{n-1,m-1})\Big) \\
&\quad +2C_V C_A\Big(v_n v_p(F_{n,m-1}F_{n-1,m-1} - F_{n-1,m}F_{n,m}) - v_m v_e(F_{n,m-1}F_{n,m} - F_{n-1,m}F_{n-1,m-1})\Big)\Big]|_{\phi=0} \\
A_{03} &= A_{30} = \\
&\quad \frac{1}{2}\Big[-(C_V^2 + C_A^2)\Big((v_e + v_p)(|F_{n,m}|^2 + |F_{n-1,m-1}|^2) + 2v_n v_m F_{n,m} F_{n-1,m-1}|_{\phi=0}\Big) \\
&\quad +2C_V C_A(1 + v_e v_p)\Big(|F_{n-1,m-1}|^2 - |F_{n,m}|^2\Big)\Big] \\
A_{13} &= A_{31} = \\
&\quad \frac{1}{2}\Big[(C_V^2 + C_A^2)\Big(v_n v_p(F_{n,m-1}F_{n-1,m-1} + F_{n-1,m}F_{n,m}) + v_m v_e(F_{n,m-1}F_{n,m} + F_{n-1,m}F_{n-1,m-1})\Big) \\
&\quad -2C_V C_A\Big(v_n(F_{n,m-1}F_{n-1,m-1} - F_{n-1,m}F_{n,m}) + v_m(F_{n,m-1}F_{n,m} - F_{n-1,m}F_{n-1,m-1})\Big)\Big]|_{\phi=0} \\
A_{02} &= -A_{20} = \\
&\quad \frac{i}{2}\Big[-(C_V^2 + C_A^2)\Big(v_n(F_{n,m-1}F_{n-1,m-1} - F_{n-1,m}F_{n,m}) + v_m(F_{n,m-1}F_{n,m} - F_{n-1,m}F_{n-1,m-1})\Big) \\
&\quad +2C_V C_A\Big(v_n v_p(F_{n,m-1}F_{n-1,m-1} + F_{n-1,m}F_{n,m}) + v_m v_e(F_{n,m-1}F_{n,m} + F_{n-1,m}F_{n-1,m-1})\Big)\Big]|_{\phi=0} \\
A_{12} &= -A_{21} = \\
&\quad \frac{i}{2}\Big[(C_V^2 + C_A^2)(1 - v_e v_p)\Big(|F_{n-1,m}|^2 - |F_{n,m-1}|^2\Big)
\end{aligned}
$$

$$
\begin{aligned}
& +2C_VC_A\Big((v_e - v_p)(|F_{n,m-1}|^2 + |F_{n-1,m}|^2) - 2v_nv_mF_{n,m-1}F_{n-1,m}|_{\phi=0}\Big)\Big] \\
A_{23} \;=\; & -A_{32} = \\
& \frac{1}{2}\Big[(C_V^2 + C_A^2)\Big(v_nv_p(F_{n,m-1}F_{n-1,m-1} - F_{n-1,m}F_{n,m}) - v_mv_e(F_{n,m-1}F_{n,m} - F_{n-1,m}F_{n-1,m-1})\Big) \\
& +2C_VC_A\Big(v_n(F_{n,m-1}F_{n-1,m-1} - F_{n-1,m}F_{n,m}) - v_m(F_{n,m-1}F_{n,m} - F_{n-1,m}F_{n-1,m-1})\Big)\Big]|_{\phi=0}, \quad (7)
\end{aligned}
$$

where $v_{n(m)} = \sqrt{2eBn(m)}$,$v_e = \frac{p_z}{\epsilon}$,and $v_p = \frac{p'_z}{\epsilon'}$. The contributions may be classified as either parity conserving($\propto (C_V^2 + C_A^2)$, symmetric) or parity violating, and by whether the parity violation occurs in the neutrino($\propto (C_V^2+C_A^2)$, anti-symmetric) or electron currents ($\propto C_VC_A$, symmetric). This last distinction is important both because the total effect of parity violating neutrino currents will tend to vanish when integrated against the initial spectrum of neutrino and anti-neutrinos, and because the asymmetric propagation of neutrinos vs anti-neutrinos will lead to asymmetries in the the star's lepton number, Y_e.

All that remains is to solve the kinematic constraints on the electron momenta and to include medium effects. The former is a straight forward algebraic exercise, yielding

$$
p_z = \frac{(Q_0^2 - Q_z^2 + 2eB(n-m))Q_z + \lambda Q_0\sqrt{(Q_0^2 - Q_z^2)^2 - 4eB(Q_0^2 - Q_z^2)(n+m) + 4e^2B^2(n-m)^2}}{2(Q_0^2 - Q_z^2)}, \tag{8}
$$

with $p'_z = Q_z - p_z$ and $\lambda = \pm 1$. Implicit in this prescription are maximum values for m and n, $N_{max} = int((Q_0^2 - Q_z^2)/2eB)$, and $M_{max} = int(\sqrt{N_{max}} - \sqrt{n})^2)$. Additionally, the integration over the energy conserving delta function will generate a Jacobian factor $|v_e - v_p|^{-1}$. After inserting Pauli blocking factors for the electron and positron, the cross section becomes

$$
\sigma = \sum_{\lambda=\pm 1}\sum_{n=0}^{N_{max}}\sum_{m=0}^{M_{max}} \frac{G_F^2 eB}{2\pi s} C_{\mu\nu}A^{\mu\nu}\frac{(1-f_e)(1-f_p)}{|v_e - v_p|} \tag{9}
$$

where $s = (k_1 + k_2)^2$ and

$$
\begin{aligned}
f_e &= \frac{1}{1 + e^{\frac{\epsilon - \mu_0}{T}}}, \\
f_p &= \frac{1}{1 + e^{\frac{\epsilon' + \mu_0}{T}}}
\end{aligned} \tag{10}
$$

with μ_0 the electron chemical potential and T the temperature of the medium.

3 Results

In order to understand the behaviour of the cross section derived in the last section, we have performed calculations for two different kinematical situations using a variety of field strengths, temperatures and densities typical of those found in astrophysical events. In the

first of these, which we shall refer to as the collinear case, the neutrino and anti-neutrino are traveling nearly parallel to one another, as is appropriate for neutrinos escaping a supernova. We assume their four momenta are given by

$$\begin{aligned} k_1 &= (E, P\sin\theta, \sqrt{s}/2, P\cos\theta) \\ k_2 &= (E, P\sin\theta, -\sqrt{s}/2, P\cos\theta) \end{aligned} \tag{11}$$

with $E = 10MeV$, and $P = 9MeV$. The second kinematical situation we shall consider is the case where the neutrino and anti-neutrino collide head-on with zero center of mass momentum. In this instance, the neutrino and anti-neutrino momenta are given by

$$\begin{aligned} k_1 &= (P, P\sin\theta, 0, P\cos\theta) \\ k_2 &= (P, -P\sin\theta, 0, -P\cos\theta). \end{aligned} \tag{12}$$

This situation, which desribes the annihilation of backscattered (anti-)neutrinos by outgoing (anti-)neutrinos, represents the largest cross section for a given incident energy. For ease of comparison with the symmetric case, we choose $P = 8.72$ MeV so that the center of mass energy, and consequently the zero field cross section, remains the same as in the case of parallel kinematics.

In both kinematical regimes, the number of possible final states grows inversely with B^2, so that it is necessary to calculate the electron-positron matrix elements for large values of n and m in order to obtain the cross section. In the case of head-on collisions, this difficulty is mitigated by the fact that only matrix elements with $n = m$ are non-zero. For the symmetric collisions, however, it is necessary to calculate Laguerre polynomials of large order. This is accomplished by upward recursion using quadruple precision arithmetic to avoid numerical instabilities. As an added precaution, the resulting polynomials have been compared to results obtained from a downward recursive Clenshaw scheme, and found to agree to six significant figures. Thus, our calculations are not limited by the accuracy to which the Laguerre functions can be realized.

In Fig. 1, the cross section for $\nu\bar{\nu} \to e^+e^-$ in free space is shown for a variety of magnetic field strengths as a function of the angle between the total momentum and the magnetic field direction, assuming symmetric kinematics for the annihilating neutrinos. The jagged structure of the cross section as a function of angle is a result of the near-vanishing of the Jacobian factor at threshold values of $\cos\theta$ where new final states for the electron-positron pair become available. For strong fields($B = 100m_e^2(\approx 4\times10^{16}\mathrm{G})$), this cross section varies strongly with angle, but this effect essentially vanishes for fields comparable to those expected in the core of superova ($B/m_e^2 < 1$). Qualitatively, the angle averaged cross section tends to decrease with increasing B, which reflects the fact that the creation of both the electron and positron in the lowest Landau level is forbidden by helicity conservation. Additionally, there is no asymmetry with respect to the magnetic field direction, as such a preference would violate CP. In Fig. 2, the cross section is shown for the head-on collisions for the same center of mass energy. Because the electron and positron are only sensitive to the total momentum of the annihilating pair, and to the direction of the B-field, the cross section

varies quadratically with the angle between the field and $\mathbf{k}_1$, and can be shown analytically to have the form

$$\sigma \propto (A_{11} + A_{33}) + \cos^2\theta(A_{11} - A_{33}) \tag{13}$$

For large magnetic fields, the A_{11} term dominates, and the annihilation cross section for neutrinos traveling parallel to the magnetic field is twice that for those traveling perpendicular to the field. As the field decreases, the electron-positron current matrix elements are more isotropic, and the angular dependence of the cross section is correspondingly smaller. Interestingly, there is a region at small fields where $A_{33} > A_{11}$, so that neutrinos traveling perpendicular to the field are more likely to annihilate.

When the neutrinos annihilate in the presence of a nearly degenerate gas of electron-positron pairs typical of the astrophysical environments, the cross section is reduced significantly by the requirement that the produced electron's energy be above the Fermi energy of the gas. Moreover, since the electron gas is not CP symmetric, the argument forbidding a parity violating asymmetry in the annihilation cross section is invalid. In Figs. 3 and 4, the cross sections for collinear and head on collisions are shown as a function of magnetic field strength, assuming an electron gas with $T = 1$ MeV and $\mu = 15$ MeV. Comparison of Figs. 1 and 3 indicates that, at the energies shown, the cross section is suppressed by a factor of 5-10, and that the cross section for annihilating pairs with momentum parallel to the magnetic field direction is larger. The suppression of the cross section for head on collisions is much more dramatic, on the order of 10^3 for the center of mass energies shown. The cross section is also observed to be more sensitive to magnetic field strength. This reflects the difficulty of producing a high energy electron in the head on collision relative to the collinear case, where the electron can be chosen to carry the bulk of the neutrinos' initial momentum. In Figs. 5 and 6, the neutrino annihilation asymmetry, defined as the ratio of the parity violating to parity conserving contributions to the cross section, as a function of magnetic field strength and direction. In the collinear case, the asymmetry is, for angles not too near 0 or π, well fit by a straight line in $\cos\theta$ with slope proportional to the strength of the magnetic field. For the head on case, the linear dependence on $\cos\theta$ can be demonstrated analytically since the electon-positron currents depend only on the total momentum perpendicular to the magnetic field. The resulting asymmetry is given by

$$R = \frac{\sigma_{PV}}{\sigma_{PC}} \propto \frac{A_{12}\cos\theta}{(A_{11} + A_{33}) + \cos^2\theta(A_{11} - A_{33})}, \tag{14}$$

with the same linear dependence on the field strength.

As we have already mentioned, the asymmetry is allowed because the background gas of electrons and positrons is not CP symmetric. Since the energies of the electrons in the magnetic field are spin dependent, there is a corresponding spin dependence in the occupation probabilities for states in a given Landau level. This variation in the occupation probabilities of states near the Fermi surface results in a preference for creating electrons with spin aligned along the field direction. In Figs. 7 and 8, the ratio of the parity violating to parity conserving contributions to the annihilation cross section is shown as a function of angle and electron chemical potential μ for $B = 10m_e^2$. For the collinear case (Fig. 7), the asymmetry increases

with μ approximately quadratically, reflecting the increase in the density of states near the Fermi surface. For the head-on case(Fig. 8), the asymmetry shows no significant dependence on μ at all. This remarkable result comes about as a result of the parity violation residing in the neutrino matrix elements, which are oblivious to the presence of the Fermi sea and to the direction of the magnetic field. Memory of the field direction is recovered when the neutrino matrix elements are multiplied by the electron currents, producing the observed asymmetry. The effect of increasing the temperature from 1-4 MeV is shown in in Figs. 9 and 10 for the same magnetic field strength. As the Fermi surface becomes more diffuse, the electron occupation numbers start to vary more slowly, with the result that the asymmetry decreases for large T. In the collinear case(Fig. 9), the asymmetry falls approximately like $\frac{1}{\sqrt{T}}$ while in the head-on kinematics the fall-off is faster, varying approximately as $\frac{1}{T}$.

Combining these results, we are able to characterize the asymmetry for the two cases in a manner that allows us to extrapolate our results to other situations. For the collinear case, we find

$$\frac{\sigma_{PV}}{\sigma_{PC}} \propto \frac{\mu^2 B}{\sqrt{T}}. \tag{15}$$

Since in this case there are two independent parameters with dimensions of energy, E and s, we have been unable to discover a simple energy dependence for the asymmetry. For the head-on case, there is only one dimensionally consistent possibility, given by

$$\frac{\sigma_{PV}}{\sigma_{PC}} \propto \frac{B}{T\sqrt{s}}. \tag{16}$$

The dependence of the head-on cross section as a function of energy and angle is shown in Fig. 11.

As we have noted previously, these relations are *approximate*, good to 10-15 per cent over a wide range of angles. Moreover, it should be apparent that these relations are only valid in instances were the asymmetry is fairly small, less than or of the order of 20 per cent. If we assume the validity of these relations, we can extrapolate from the relatively high fields($\approx 10^{14}$ G) where calculations are feasible, to the field strengths observed in pulsars($\approx 10^{12}$G)[14]. The result of this scaling is an asymmetry of order 10^{-4}, which is significantly smaller than that required to produce the observed recoil velocities of neutron stars. The smallness of this result does not, however, rule out neutrino asymmetries as a source of the recoil velocities since the relatively small asymmetries produced by neutrino annihilations may be amplified by hydrodynamic instabilities in the collapsing core[15]. Additionally, there have been speculations that much larger magnetic fields may exist[16][17]. Finally, it should be noted that there are other neutrino processes for which the cross section and asymmetries may be larger, and multiple neutrino interactions may significantly increase the net asymmetry[18].

In summary, we have calculated the cross section for $\nu\bar{\nu} \rightarrow e^+e^-$ in the presence of a magnetic field for an extensive set of conditions typical of those found in astrophysical environments. We do not find that the presence of the field provides any significant enhancement of the cross section at fixed chemical potential. Although the presence of a degenerate gas

of electrons provides the possibility of parity violation in this reaction, they are insufficient to produce the observed recoil velocities of neutron stars at the field strengths known to be associated with pulsars.

Acknowledgments

This authors wish to acknowledge support from NSF Research Contract No. PHY-9408843 and DOE grant DE-FG02-87ER40365.

References

[1] *Supernovae*, edited by A. Petschek, Springer-Verlag, New York, 1990,
M. Ruffert, H.-Th. Janka, K. Takahashi and G. Schaefer, Astron. Astrophys. **319**, 122(1997).

[2] S. Colgate, Nature **341**,489(1989).

[3] H.-Th. Janka and M. Ruffert, astro-ph9512144.

[4] H.-Th. Janka, Astron. Astrophys.**244**, 378(1991).

[5] S. L. Adler and C. Schubert, Phys. Rev. Lett. **77**(1996)1695, V. N. Bainer, A. I. Milstein and R. ZhShaisultanov, Phys. Rev. Lett. **77** (1996) 1691.

[6] A.V. Kuznetsov and N.V. Mikheev, hep-ph 9612312, submitted to Phy. Lett. B.

[7] V.G. Bezchastnov and P. Haensel, astro-ph 9608090, submitted to Phys Rev D.

[8] A.D. Kaminker, K.P. Levenfish, D.G. Yakolev, P. Amsterdamski, and P. Haensel, Phys. Rev. **D46**, 3256(1992),
P. Amsterdamski and P. Haensel, Phys. Rev. **D42**, 2915(1990).

[9] A. Vilenkin, Ap. J**451**, 700(1995),
N. N. Chugai, Sov. Astron. Lett. **10**,87(1984),

[10] C.J. Horowitz and J. Piekarewicz, astro-ph/9701214.

[11] A.G. Lyne and D. R. Lorimer, Nature **369**, 127(1994).

[12] M. Abramowicz and I. Stegun, *Handbook of Mathematical Functions*, Dover Publications, New York, 1968.

[13] A.D. Kaminker and D.G. Yakolev. Teor. Mat. **49**, 248(1981).

[14] V.S. Beskin, A. V. Gurevich, and Ya. N. Istomin, Physics of the Pulsar Magnetosphere, Cambridge Univ. Press, Cambridge 1993.

[15] Herant et. al., Ap. J**435**, 339(1994).

[16] C. Tomson and R.C. Duncan, Mon. Not. R. Astron. Soc., **275**, 757(1995).

[17] E. Mueller and Hillebrandt, Astron. Astrophys. **80**, 147(1979).

[18] C.J. Horowitz and Gang Li, astro-ph/9705126, IUNTC 97-03.

<u>Figure Captions</u>

- Fig. 1 - Neutrino annihilation cross section in free space for collinear kinematics as a function of magnetic field strength(in units of m_e^2) and direction of the neutrino pair's total momentum.
- Fig. 2 - Neutrino annihilation cross section in free space for head-on collisions as a function of magnetic field strength(in units of m_e^2) and direction of the neutrino's momentum.
- Fig. 3 - Neutrino annihilation cross section(collinear kinematics) at astrophysically interesting temperature($T = 1$ MeV) and density($\mu = 15$ MeV) as a function of magnetic field strength(in units of m_e^2) and direction of the neutrino pair's total momentum.
- Fig. 4 - Neutrino annihilation cross section(head-on kinematics) at astrophysically interesting temperature($T = 1$ MeV) and density($\mu = 15$ MeV) as a function of magnetic field strength(in units of m_e^2) and direction of the neutrino's momentum.
- Fig. 5 - Neutrino annihilation asymmetry for the collinear case as a function of magnetic field strength and the direction of the neutrino pair's total momentum. The electron temperature and density are the same as in Fig. 4.
- Fig. 6 - Neutrino annihilation asymmetry for head on collisions as a function of magnetic field strength and the neutrino's momentum. The electron temperature and density are the same as in Fig. 4.
- Fig. 7 - Neutrino annihilation asymmetry for the collinear case as a function of chemical potential and the direction of the neutrino pair's total momentum. The electron temperature is the same as in Fig. 4, and the magnetic field strength is $B = 10m_e^2$.
- Fig. 8 - Neutrino annihilation asymmetry for head on collisions as a function of chemical potential and the direction of the neutrino's momentum. The electron temperature is the same as in Fig. 4, and the magnetic field strength is $B = 10m_e^2$.
- Fig. 9 - Neutrino annihilation asymmetry for the collinear case as a function of temperature and the direction of the neutrino pair's total momentum. The electron chemical potential the same as in Fig. 4, and the magnetic field strength is $B = 10m_e^2$.
- Fig. 10 - Neutrino annihilation asymmetry for head on collisions as a function of temperature and the direction of the neutrino's momentum. The electron chemical potential is the same as in Fig. 4, and the magnetic field strength is $B = 10m_e^2$.
- Fig. 11 - Neutrino annihilation asymmetry for head on collisions as a function of neutrino center of mass energy and the direction of the neutrino's momentum. The electron chemical potential and temperature are the same as in Fig. 4, and the magnetic field strength is $B = 10m_e^2$.

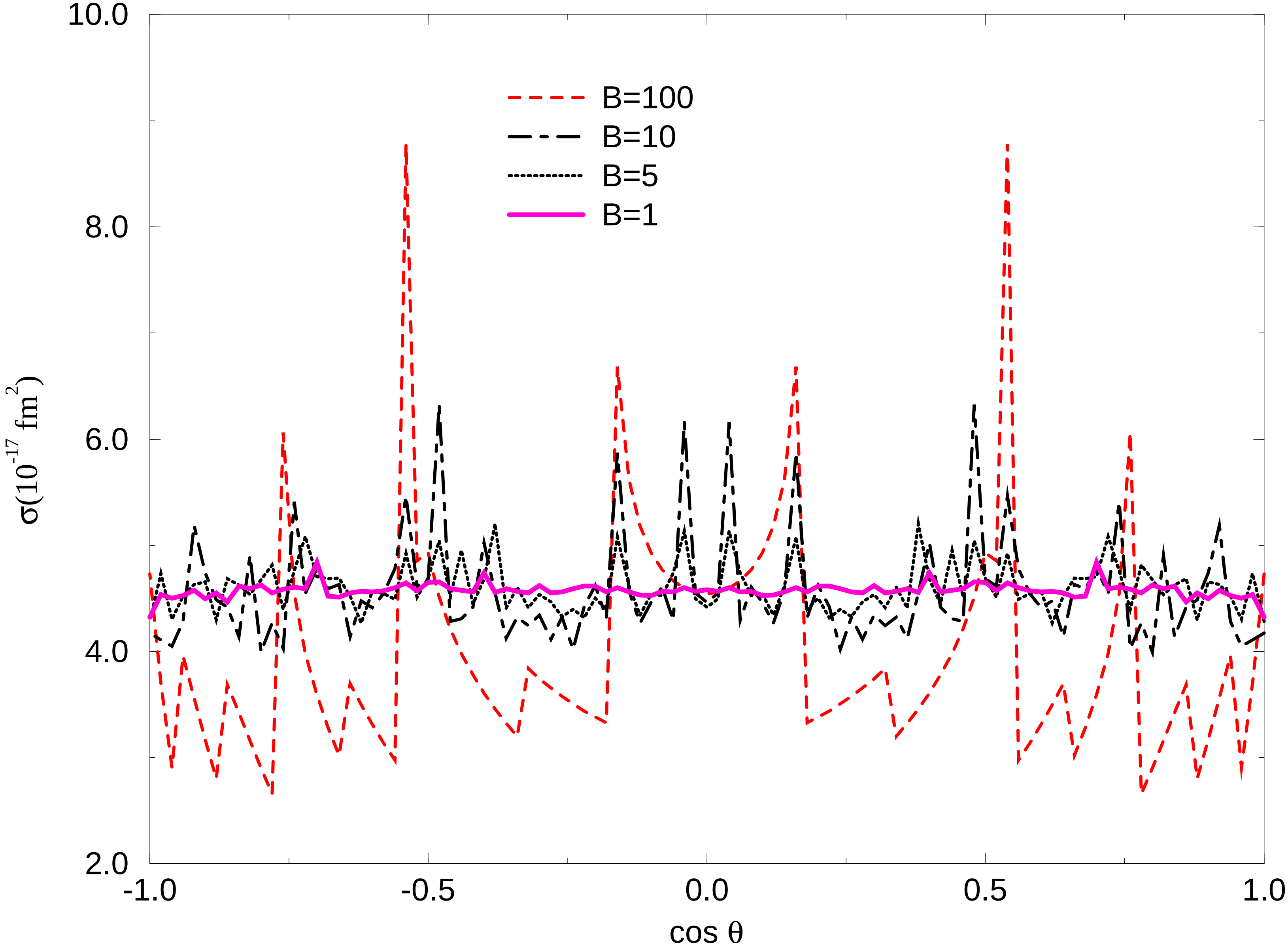

10.0
8.0
6.0
4.0
2.0
-1.0
-0.5
0.0
0.5
1.0
cos θ
σ(10^-17 fm^2)
B=100
B=10
B=5
B=1

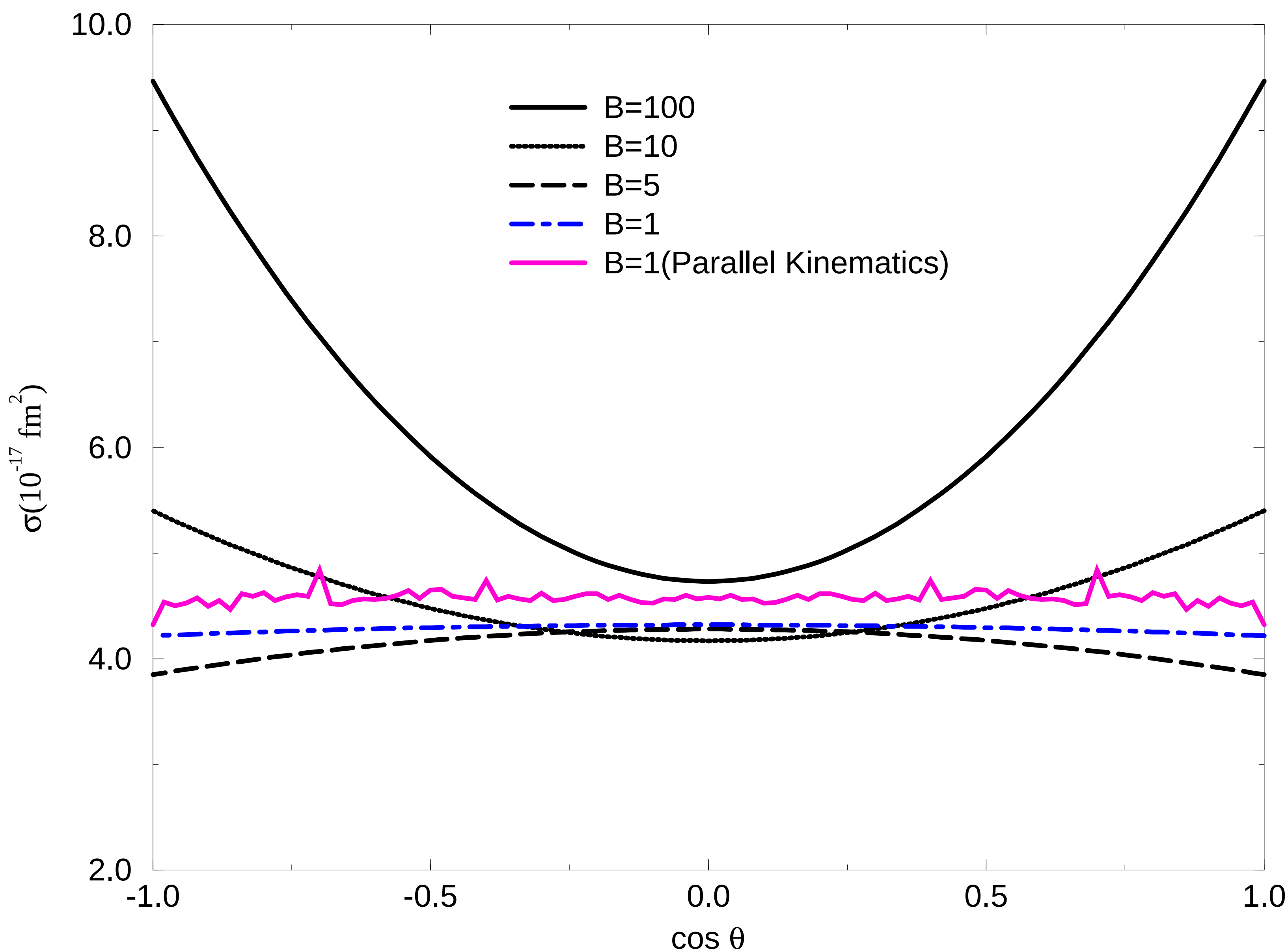

10.0
8.0
6.0
4.0
2.0
-1.0
-0.5
0.0
0.5
1.0
cos θ
σ(10^-17 fm^2)
B=100
B=10
B=5
B=1
B=1(Parallel Kinematics)

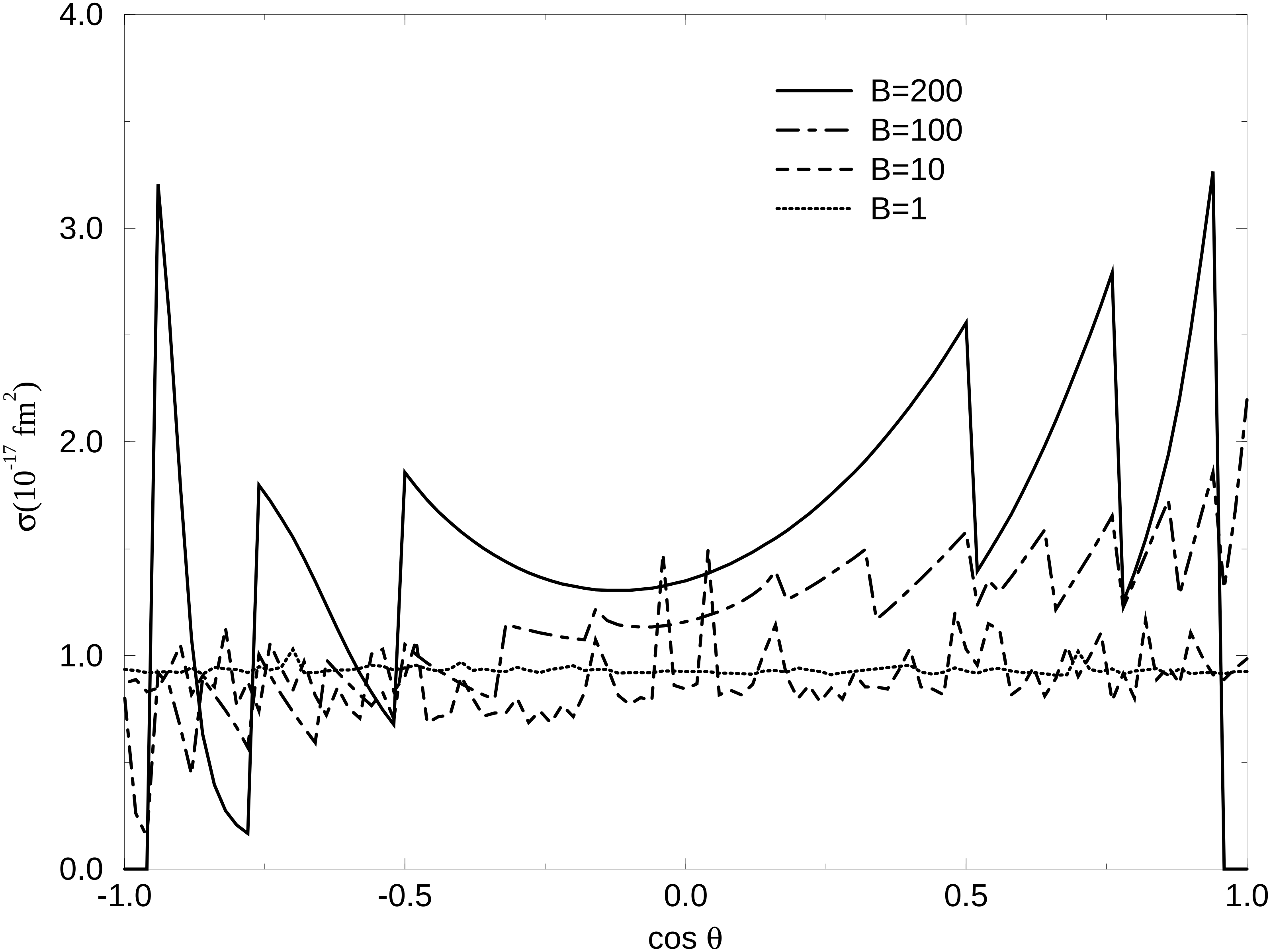

4.0
3.0
2.0
1.0
0.0
-1.0
-0.5
0.0
0.5
1.0
σ(10^-17 fm^2)
cos θ
B=200
B=100
B=10
B=1

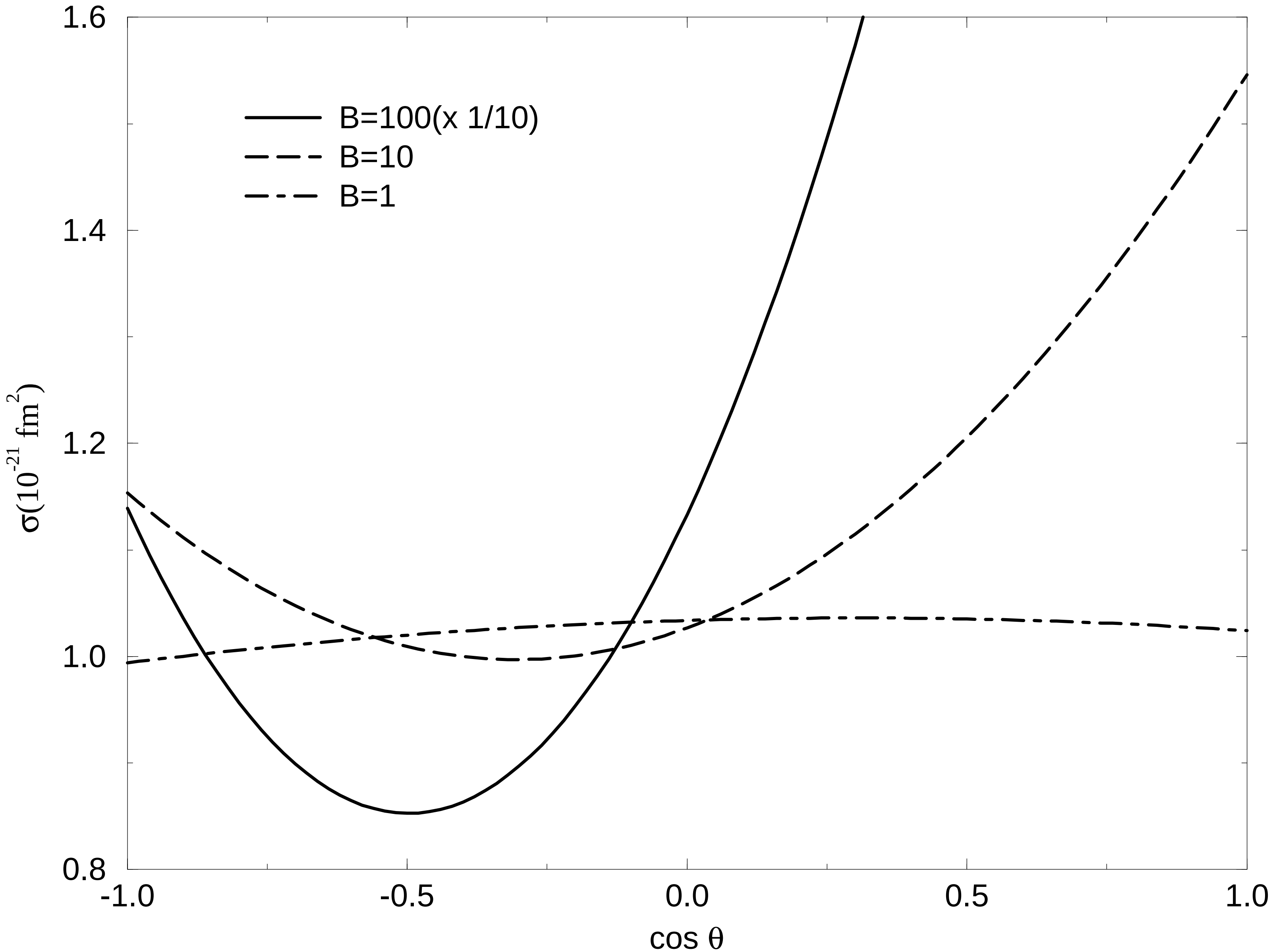

1.6
1.4
1.2
1.0
0.8
-1.0
-0.5
0.0
0.5
1.0
cos θ
σ(10^-21 fm^2)
B=100(x 1/10)
B=10
B=1

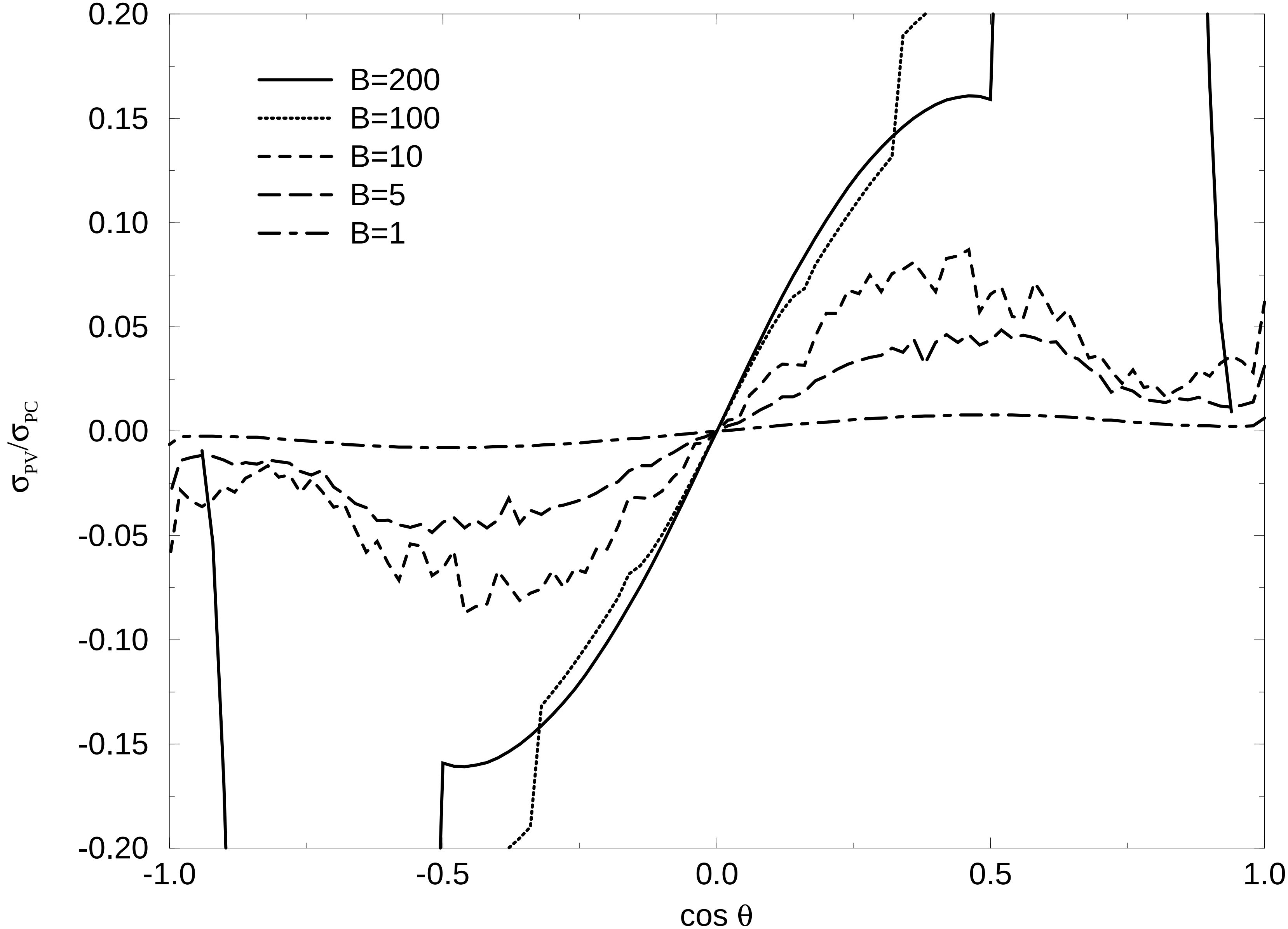
B=200
B=100
B=10
B=5
B=1
0.20
0.15
0.10
0.05
0.00
-0.05
-0.10
-0.15
-0.20
-1.0
-0.5
0.0
0.5
1.0
cos θ
σPV/σPC

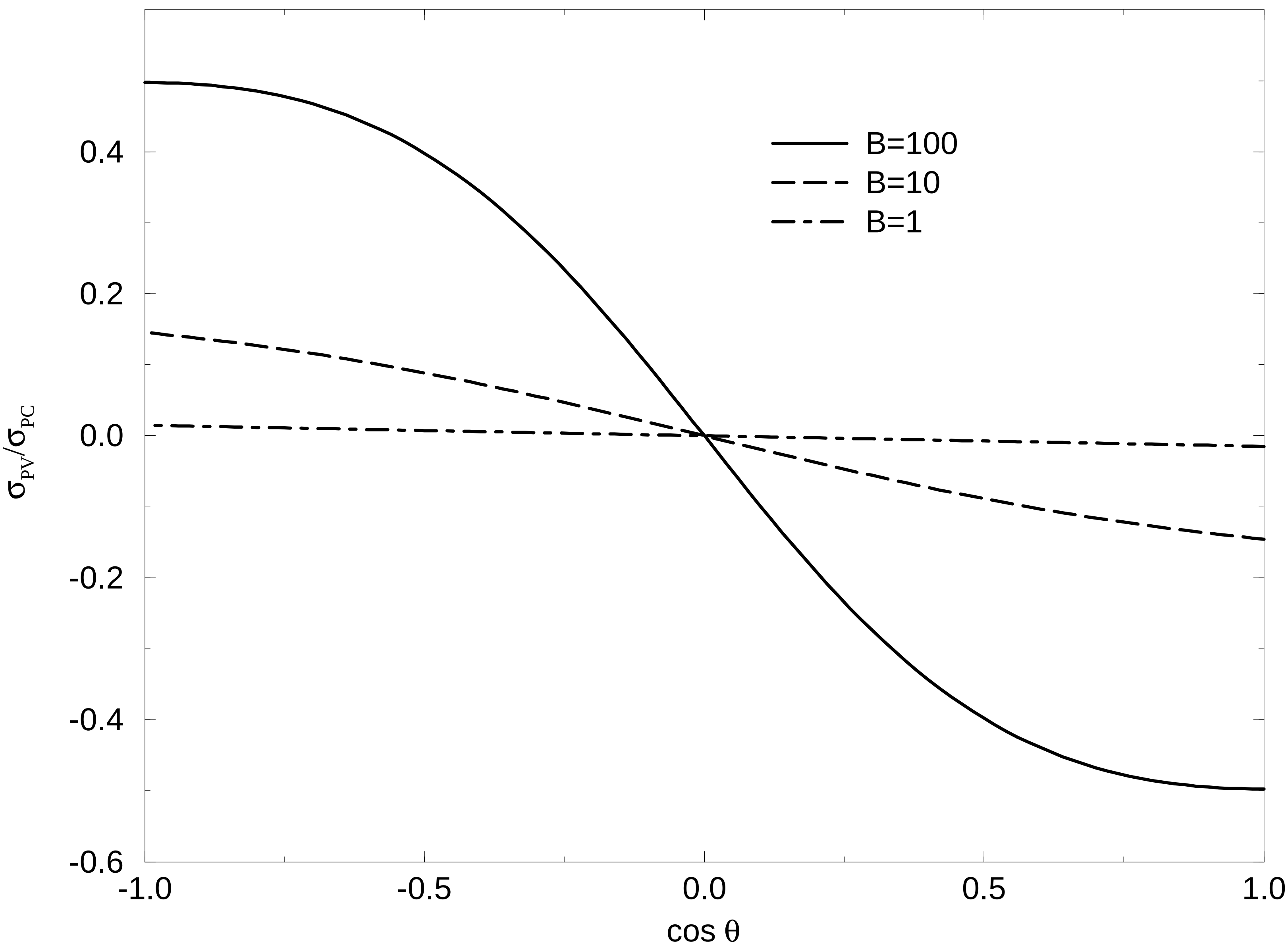
B=100
B=10
B=1
0.4
0.2
0.0
-0.2
-0.4
-0.6
-1.0
-0.5
0.0
0.5
1.0
cos θ
σ_{PV}/σ_{PC}

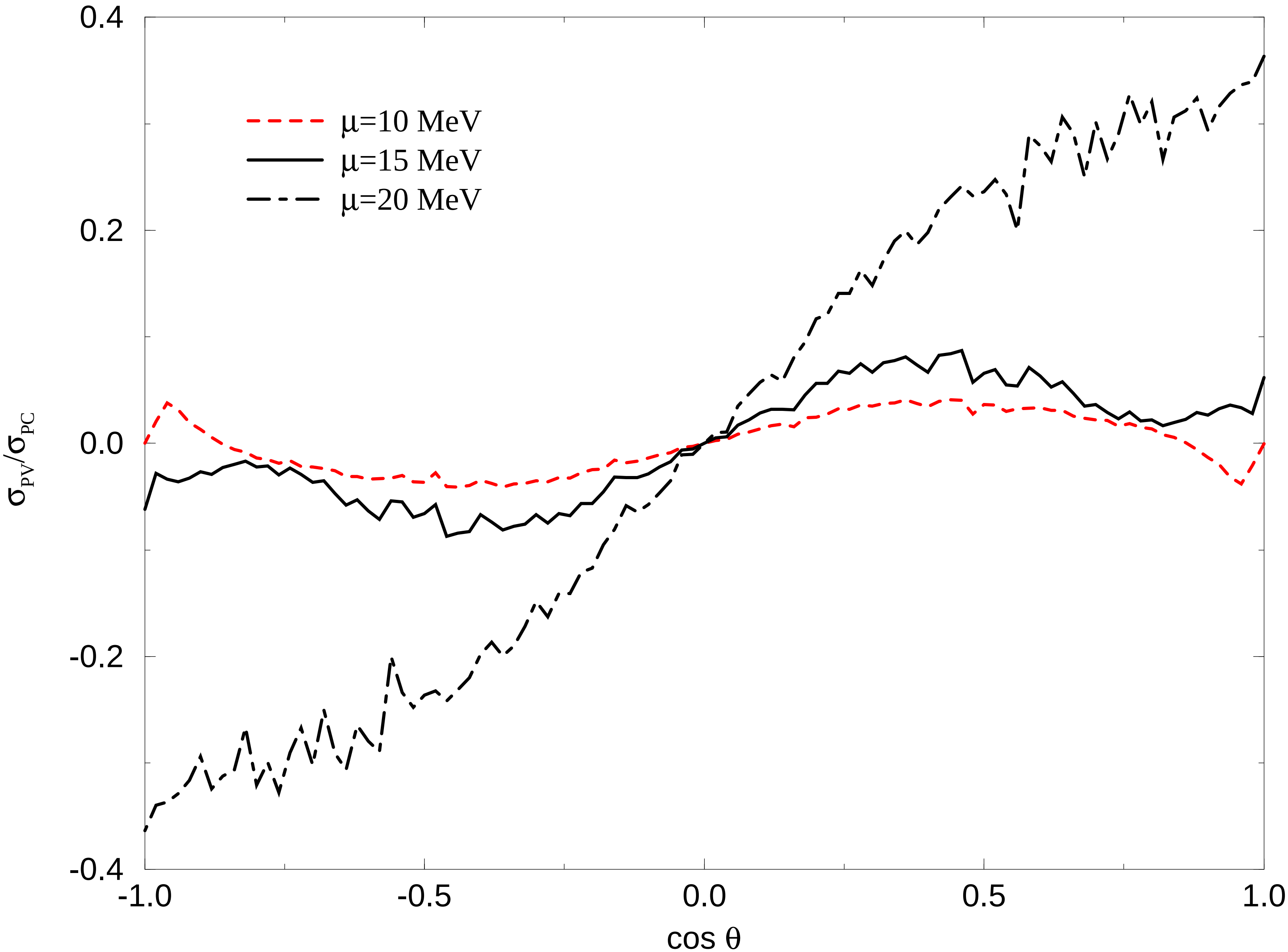

μ=10 MeV
μ=15 MeV
μ=20 MeV
0.4
0.2
0.0
-0.2
-0.4
-1.0
-0.5
0.0
0.5
1.0
cos θ
σPV/σPC

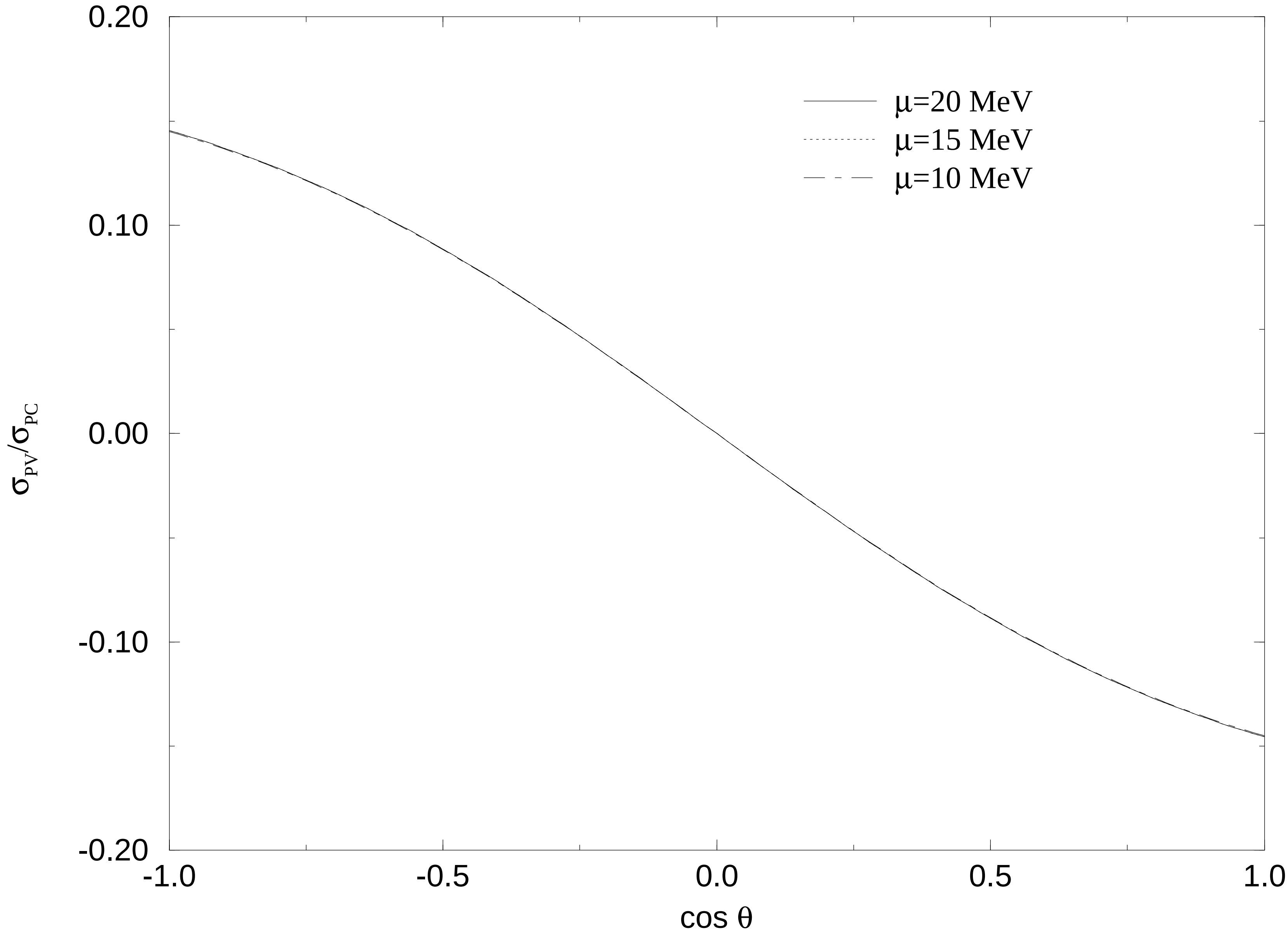

0.20
0.10
0.00
-0.10
-0.20
-1.0
-0.5
0.0
0.5
1.0
cos θ
σPV/σPC
μ=20 MeV
μ=15 MeV
μ=10 MeV

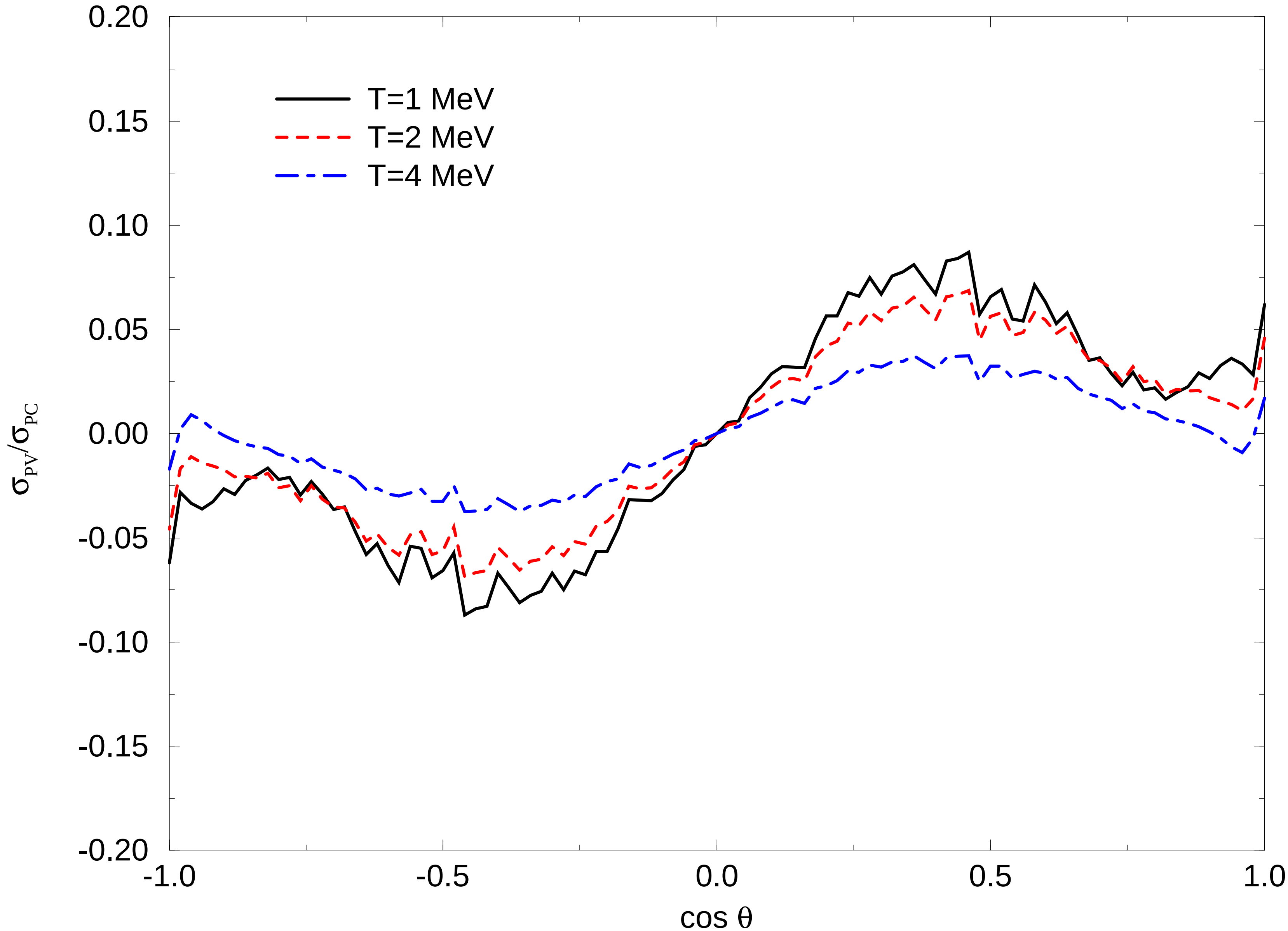

0.20
0.15
0.10
0.05
0.00
-0.05
-0.10
-0.15
-0.20
-1.0
-0.5
0.0
0.5
1.0
T=1 MeV
T=2 MeV
T=4 MeV
σ_{PV}/σ_{PC}
cos θ

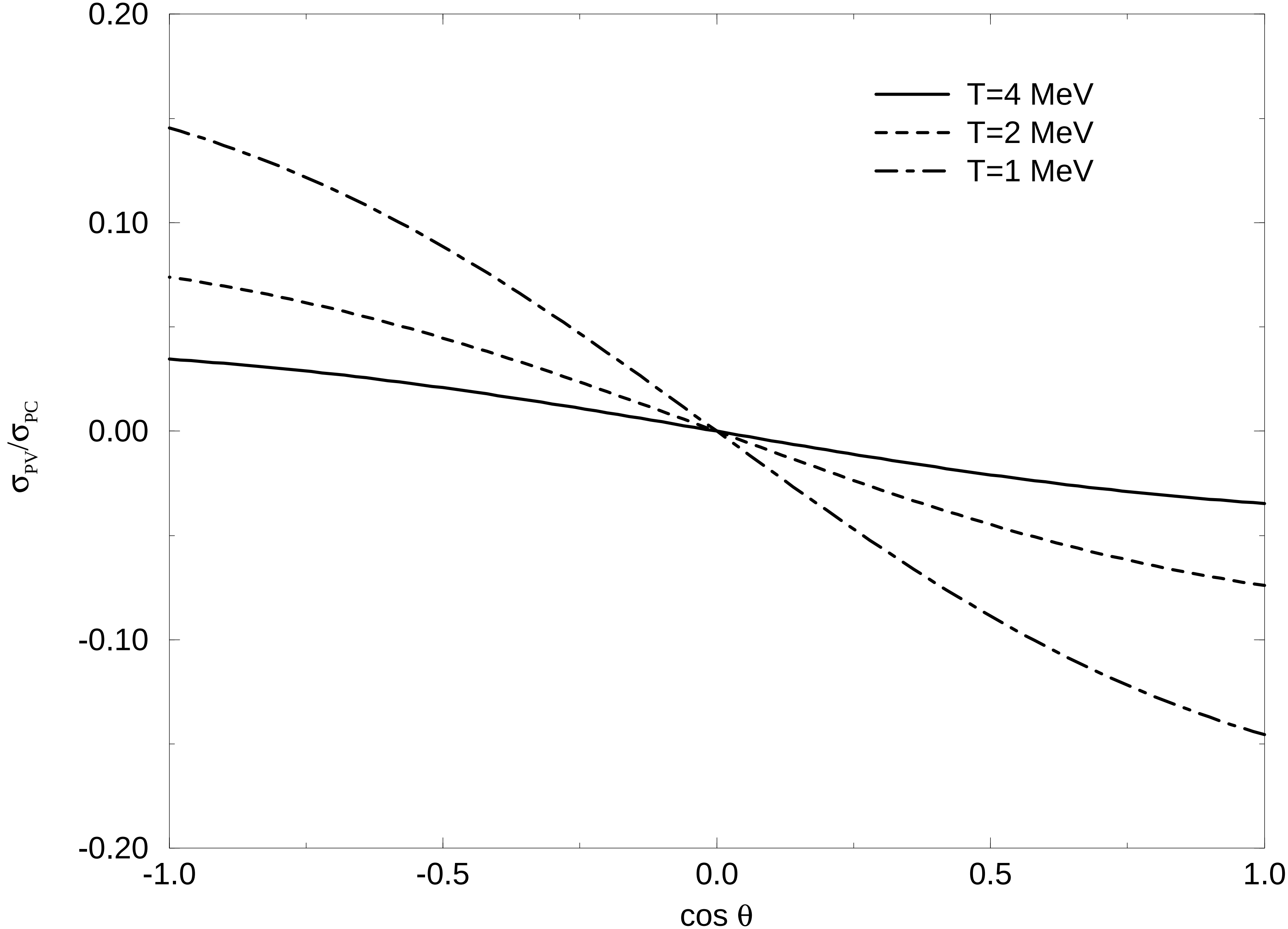

T=4 MeV
T=2 MeV
T=1 MeV
0.20
0.10
0.00
-0.10
-0.20
-1.0
-0.5
0.0
0.5
1.0
cos θ
σPV/σPC

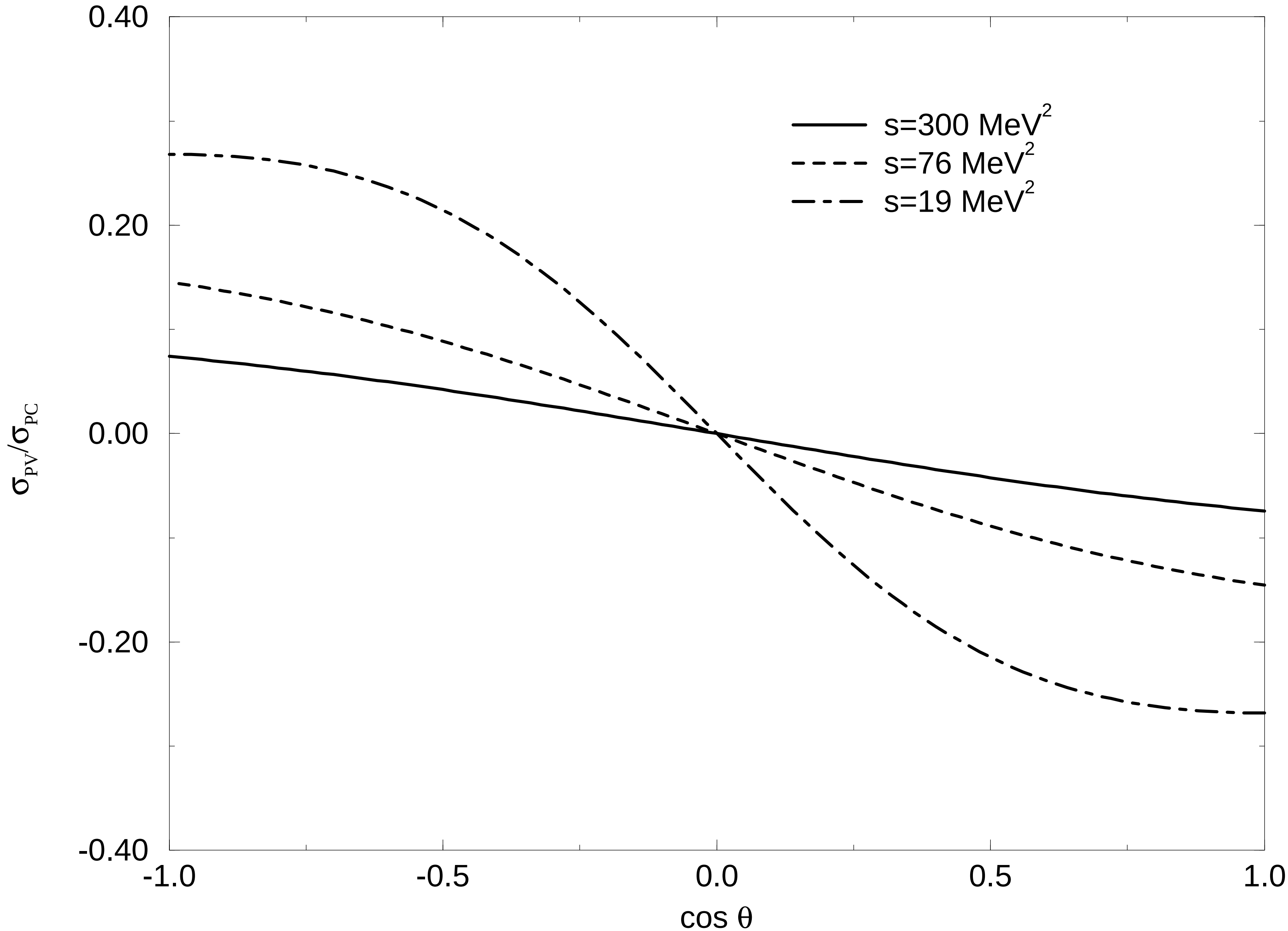

0.40
0.20
0.00
-0.20
-0.40
-1.0
-0.5
0.0
0.5
1.0
cos θ
σ_PV/σ_PC
s=300 MeV^2
s=76 MeV^2
s=19 MeV^2